IEEE Access
Multidisciplinary | Rapid Review | Open Access Journal

Received May 15, 2020, accepted June 10, 2020, date of publication June 15, 2020, date of current version June 24, 2020.

Digital Object Identifier 10.1109/ACCESS.2020.3002206

FoV-Based Quality Assessment and Optimization for Area Coverage in Wireless Visual Sensor Networks

THIAGO C. JESUS[1,2], DANIEL G. COSTA[1], (Senior Member, IEEE), PAULO PORTUGAL[2], (Member, IEEE), AND FRANCISCO VASQUES[2]

[1]Department of Technology, State University of Feira de Santana, Feira de Santana 44036-900, Brazil
[2]Faculty of Engineering, INEGI/INESC-TEC, University of Porto, 4200-465 Porto, Portugal

Corresponding author: Thiago C. Jesus (tcjesus@uefs.br)

This work was a result of the project Operation NORTE-08-5369-FSE-000003 supported by Norte Portugal Regional Operational Programme (NORTE 2020), under the PORTUGAL 2020 Partnership Agreement, through the European Social Fund (ESF). Additionally, this work was also partially funded by the Brazilian CNPq (Conselho Nacional de Desenvolvimento Científico e Tecnológico) Agency under Grant 204691/2018-4.

ABSTRACT Wireless visual sensor networks are commonly employed on several applications contexts such as smart cities, intelligent transportation systems and industrial management, aiming at the use of visual data from cameras to provide enhanced information and to expand the networks utilities. In these scenarios, some applications may require high-definition images when performing more specialized tasks, for example in face and text recognition, adding an important monitoring requirement when using camera-based sensors. In fact, it is important to ensure that the network is able to gather visual data with the associated required quality to each task, and such perceived quality may be processed as a function of the Field of View (FoV) of the visual sensors. In order to address this issue, new quality metrics are proposed for wireless visual sensor networks that are deployed to perform area coverage, exploiting for that different perceptions of the FoV. Those metrics are proposed along with redeployment optimization methods for visual sensor nodes aiming at the improvement of the perceived monitoring quality, which are based on greedy and evolutionary-based approaches. The proposed metrics and algorithms are expected to be more realistic than previous solutions, allowing flexible processing of variables as cameras' positions, orientations and viewing angles, providing then high flexibility on the definition of parameters and significantly contributing to the development of sensor networks based on visual sensors.

INDEX TERMS Wireless sensor networks, area coverage, optimization, visual quality, quality of monitoring, quality metric, visual sensing, field of view, mathematical modelling.

I. INTRODUCTION

Several applications have benefited from the use of distributed systems and visual information when achieving a more comprehensive perception of the monitoring context, usually employing (Wireless) Visual Sensor Networks (WVSN) composed of a set of camera-enabled nodes [1]. For those networks, retrieved visual information must be adequate to the application monitoring requirements, *i.e.*, the proper visual data "quality" is essential to perform the expected tasks. However, the definition of quality is subjective and it may vary considerably, making harder the definition of quality assessment metrics.

Nevertheless, such metrics could be an important requirement to develop and manage some applications in any context, such as in Industrial 4.0 [2], environmental monitoring [3], mobility tracking [4], Internet of Things [5] or just for network metric analysis, such as in dependability assessment [6].

Actually, when considering the use of visual sensor networks, some tasks will demand a stronger perception of quality, for example requiring the adjustment of the position or orientation of cameras in order to enhance the quality of retrieved visual data, taking closer and sharper images of objects. Similarly, more powerful hardware may be used to

The associate editor coordinating the review of this manuscript and approving it for publication was Yong Yang.

gather better images, also impacting quality [7]. On the other hand, some monitoring tasks may not require high-definition images, such as in intrusion detection applications that essentially need to detect movement patterns. For this last case, it is possible to save resources or use cheaper hardware in order to perform simpler monitoring tasks, while achieving acceptable results. Such scenario, with applications with different demands concerning the quality of retrieved visual data, is susceptible to the adoption of quality metrics that leverage the processing and resource allocation in such networks.

It is important to distinguish between quality of image [8]–[11] and Quality of Monitoring (QoM) [12]–[16] in a visual network. The image quality assessment evaluates the image content degradation as consequence of acquisition, processing, compression, storage, transmission and reproduction processes. On the other hand, quality of monitoring is a generic term used to refer to the capability of a network to perform the expected monitoring functions over the region of interest. In this case it is assessed the value of gathered visual information not considering content degradation, although it is possible to join both approaches for a more realistic assessment. In this paper it is discussed assessment of quality of monitoring on wireless visual sensors networks only.

Still considering the relevant aspects for quality of visual monitoring, several networks aspects like area coverage and redundancy [17], [18] can affect the perceived quality, which means that it can be indirectly used to evaluate other metrics. It can also determine other network attributes such as dependability, availability, lifetime or power consumption [15], [19], which means that a proper quality mapping could also be used to improve other network features or even to prevent and identify failures [20].

In previous works in the literature [21]–[23], some QoM metric is usually exploited according to the sensors ability to view one or more targets. However, it is also possible to define a QoM for area coverage applications [24], which is a more challenging task since there are no reference points with respect to the camera. Instead, the regions expand continuously, varying both in distance and perspective from each visual sensor node. Moreover, some regions may be redundantly covered by several visual nodes, increasing the complexity of area coverage. For these cases, it makes more sense to define a metric to the entire network considering the composition of covered areas.

The problem of quality of monitoring regarding area coverage was initially addressed in [24], but imposing several restrictions to the network deployment (position, orientation, viewing angle) and, as a consequence, to the network optimization process. In a different way, in this article we circumvent these constraints proposing a new approach for assessment of the quality of monitoring in WVSN, defining new QoM-based metrics. The proposed metrics, defined as the Area Quality Metric (AQM) and its variations, are types of QoM metrics that can be used for optimizations, comparisons or exploitation of different quality aspects, such as redundancy and dependability. In fact, in this work, the proposed metrics are used to guide the network redeployment based on QoM-based optimizations. For this purpose, we also propose three optimization methods (Greedy, Pseudo-Greedy and Evolutionary - Genetic Algorithm) and compare their results in terms of quality improvement. The model is more realistic than others found in literature since it does not consider predefined cameras' position or orientation (neither on deployment or on redeployment) and provides support to heterogeneous hardware configuration. For the best of our knowledge, no metric and optimization algorithms with these objectives have been proposed before.

The remainder of the article is organized as follows. Section II presents some related works regarding coverage and quality in Wireless Sensor Networks (WSN). Some fundamental concepts are presented in Section III. Then, three quality metrics are proposed and discussed in Section IV. The proposed optimization algorithms are described in Section V, detailing the ideas behind the greedy, pseudo-greedy and evolutionary approaches. Section VI presents and discusses the results for some WVSN scenarios. Finally, the conclusions are stated in Section VII.

II. RELATED WORKS

Quality of monitoring in wireless sensor networks has been addressed in different contexts in the literature. When concerning visual sensing, the most common approaches are related to targets coverage, comprising both scalar and directional sensors. Some of the most relevant works are then discussed in this section, giving important clues of how quality of monitoring has been assessed and optimized in visual sensor networks.

In [15], authors aim to find a scheduling approach for scalar sensors in order to maximize the target coverage quality. In this case, it is explicitly proposed a QoM metric for targets, measuring the number of time slots in which targets are covered, considering the amount of energy consumed by each sensor during the monitoring period.

Similarly, the authors in [14] also use the concept of QoM to provide an efficient sensor scheduling, selecting the active sensors based on the QoM of the sensors related to the desired targets. However, in that work, QoM is calculated for each single sensor, considering the ratio of the distance between the sensor and target to the sensing range. Although the authors approach directional sensors, they focus specifically in ultrasonic and infrared sensors, which present a different notion of QoM. Hence, that method only considers one sensor active at time, and consequently it does not provide a QoM metric for the entire network.

The distance of a target point to a sensor is also considered to determine a perception of QoM in [16], but in visual networks, which means that the directional sensors are cameras. A QoM metric is defined and used to guide the network deployment based on a predefined set of discrete feasible configurations for all camera types.

In [25], QoM in visual networks is also addressed, also considering target coverage, but exploiting the fact that the quality of visual information is sensitive to its viewpoint. That way, the authors address full view coverage considering target viewing related to target facing direction and the viewed direction of the objects, which reflects the viewpoint of a sensor. However, the perception of QoM is assumed as a condition to select a non-faulty sensor node instead of being considered as a metric.

Still considering visual networks for target coverage, the authors in [13] consider an anisotropic monitoring due to the perspective of monitored objects in relation to the cameras. In that work, the cameras can assume any orientation and position, since they are attached to unmanned aerial vehicles (UAV).

In [24] the notion of QoM in visual networks is discussed for area coverage. The authors consider the weighted sensing quality and the importance of sensing area to establish Quality of Monitoring in a full coverage scenario. That work focuses on the network deployment (position, orientation, viewing angle) and, as a consequence, it can support an eventual network optimization process. However, coverage redundancy is not clearly discussed in that paper, providing inconsistent understanding about QoM calculation.

In this article we discuss and propose new QoM metrics for quality assessment when performing area coverage by visual sensor networks, without restrictions to cameras' orientations, positions or viewing angles. Such metrics are expected to be meaningful for single visual sensor nodes or even for an entire network. Moreover, we show how to use these metrics to improve the QoM perception of the network using different optimization methods, in a flexible and broader perspective. Putting all these together, this article brings important contributions to the area, which were not proposed before.

III. DEFINITIONS AND BASIC CONCEPTS

In this article, we follow the visual coverage formulation presented in [21] and [26], taking their mathematical models as reference. Table 1 lists the notations we use in this paper. In the defined problem scope, it is considered a set of visual sensors, $VS = \{vs_1, vs_2, \ldots, vs_n\}$, which are deployed over a two-dimensional area $\mathbb{A}$. Each sensor $vs \in VS$ is located using Cartesian coordinates and it is expected to be equipped with a camera, having a viewing angle θ_{vs} and an orientation α_{vs}, as shown in Figure 1, where the camera is represented by the small red circle. Each camera also presents a sensing radius R_s as the approximation of the camera's Depth of Field (DoF), which is the region between the nearest and farthest point that can be sharply sensed [27]. Each camera may assume different values for their parameters, however, without loss of generality, we consider in this work that all visual sensors are identical and so they are configured with the same values. For simplification and in order to make this problem tractable and computationally feasible when employing WSN in real applications, sensor nodes should be assumed as having limited hardware processing resources and low-power requirements [21].

TABLE 1. Adopted notations.

Symbol	Meaning
vs_i	i-th visual sensor node
θ_{vs}	Viewing angle of a visual sensor node
α_{vs}	Orientation of a visual sensor node
R_s	Camera's sensing radius
FoV_{vs}	Field of view of a visual sensor node
$\mathbb{A}$	Monitoring field
MA	Monitoring area
w, h	Width and height of the monitoring area, respectively
β	Rotation angle of the monitoring area
mb	Monitoring block
ws, hs	Width and height of a monitoring block, respectively
M, N	Number or columns and rows of monitoring blocks grid
CA_{mb}	Coverage area considering MBs viewed
FoV_{vs}^{li}	Field of view of i-th quality level of vs
dov_i	Distance of view of i-th quality level
w_i	Weight value of i-th quality level
$w_{\max}$	Maximum weight of a MB among sensors covering it
AQM	Area quality metric
AQM_{rel}	Relative area quality metric
AQM_{abs}	Absolute area quality metric
O_{vs}	Set of Greedy sectors
γ_{sec}	Angle of a Greedy sector
α_{vs}^{o}	A possible new orientation of vs on redeployment

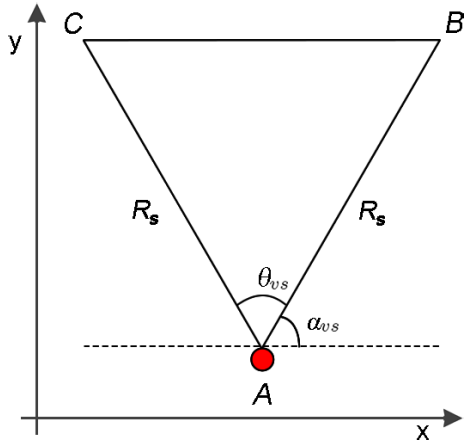

FIGURE 1. Field of View of a visual sensor.

The Field of View (FoV) of any visual sensor is defined as the area of an isosceles triangle composed of three vertices, A, B and C (see Figure 1), being (A_x, A_y) the Cartesian coordinates of the sensor. The coordinates of vertices B and C can be calculated by Equation 1 and the FoV of any visual sensor vs_i is the area of the triangle $\triangle ABC$, which can be computed using trigonometry, as expressed in

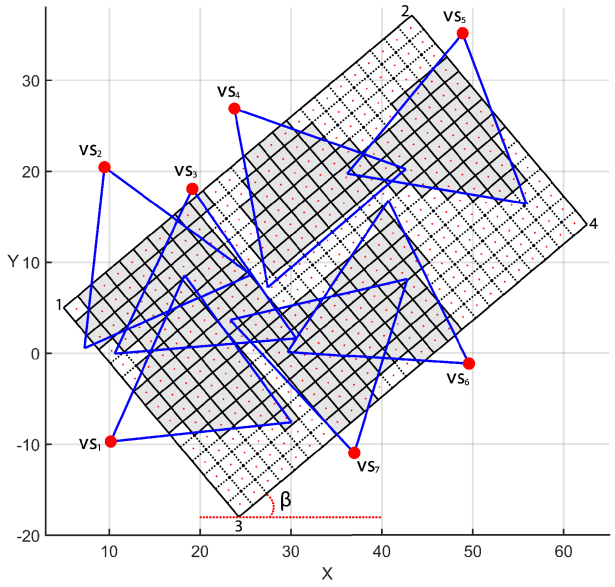

FIGURE 2. Monitoring area being covered by visual sensor nodes vs_i, $i = 1, \ldots, 7$.

Equation 2 [21].

$$\begin{aligned} B_x &= A_x + R_s \cos(\alpha_{vs}) \\ B_y &= A_y + R_s \sin(\alpha_{vs}) \\ C_x &= A_x + R_s \cos((\alpha_{vs} + \theta_{vs}) \bmod 2\pi) \\ C_y &= A_y + R_s \sin((\alpha_{vs} + \theta_{vs}) \bmod 2\pi) \end{aligned} \quad (1)$$

$$FoV_{vs} = \frac{R_{vs}^2 \cdot \sin(\theta_{vs})}{2} \quad (2)$$

The monitoring field $\mathbb{A}$ on which a WVSN operates can characterize different regions, such as an industrial plant, a military field, a public square, an avenue, an entire city or even a farm. Whatever the case, a monitoring field may be composed by one or more Monitoring Areas (*MA*), each one described as a rectangle defined by its origins $(x1, y1)$, a width w, a height h and a rotation angle β, as shown in Figure 2. The other vertices of a *MA* can be computed in a 2*D* Cartesian plan, as presented in Equation 3.

$$\begin{aligned} x2 &= x1 + w.\cos(\beta) \\ y2 &= y1 + w.\sin(\beta) \\ x3 &= x1 + h.\sin(\beta) \\ y3 &= y1 - h.\cos(\beta) \\ x4 &= x1 + h.\sin(\beta) + w.\cos(\beta) \\ y4 &= y1 - h.\cos(\beta) + w.\sin(\beta) \end{aligned} \quad (3)$$

A *MA* is the area of interest of a visual application and only visual information from this sub-region is relevant to the considered WVSN. If necessary, a non-rectangular monitoring area can be defined as the union of t smaller *MAs*, as shown in Figure 3, for instance. In other words, $MA = MA_1 \cup MA_2 \cup \cdots \cup MA_t$, such as $\bigcap_{i=1}^{t} (MA_i) = \emptyset$.

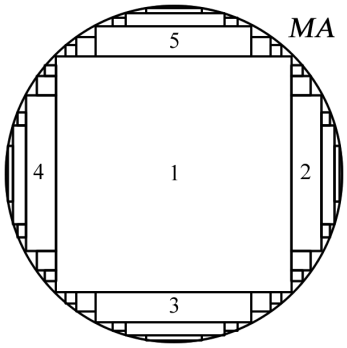

FIGURE 3. A non-rectangular monitoring area represented by the union of several rectangles.

In that case, a circular monitoring area can be represented by several rectangles, each one defining a single monitoring area. The resulting *MA* will be more realistic if the empty spaces are fulfilled with more or even smaller rectangles.

A single *MA* can be divided in smaller regions, called Monitoring Blocks (*MB*), each one defined as rectangles represented by its origins $(x1s, y1s)$, a width ws, a height hs and a center (xc, yc). Thus, a MA is composed by a grid of monitoring blocks with size $M \times N$. In this case, the "area coverage" problem can be indirectly approached as several "target coverage" problems, where each point (xc, yc) is a target with infinitesimal size. This is an important abstraction aimed at higher efficiency, while keeping the computational cost low, as we previously discussed in [28]. In that paper, the monitoring blocks approach for area calculation has been proven to be a good approximation in terms of accuracy, with low computational cost.

We consider that a single monitoring block mb is covered by a visual sensor node vs if the center mb (xc, yc) is inside the polygon area of FoV_{vs}. In this configuration, the Monitoring Block is assumed to be covered as a whole, and its area $ws \times hs$ is counted to the total coverage area [27], [28]. We represent a covered *MB* with the notation $mb \in FoV_{vs}$. This definition can be extended for a set of visual sensors *VS* according to Equation 4. In this paper it is not considered the impact of perspective from cameras in area coverage, *i.e.*, it makes no difference here to cover a *MB* from different angles.

$$cover(mb, VS) = \begin{cases} 1, & \text{if } \exists vs \in VS \mid mb \in FoV_{vs} \\ 0, & \text{otherwise} \end{cases} \quad (4)$$

The total area covered by *VS* is the product of the area of a single *MB* by the quantity of monitoring blocks covered by at least one visual sensor, according to Equation 5.

$$CA_{mb}(VS) = ws \cdot hs \cdot \sum_{j=1}^{M} \sum_{l=1}^{N} cover\left(mb_{j,l}, VS\right) \quad (5)$$

Besides the coverage area, another important aspect related to visual sensor networks is the subjective perception of Quality of Monitoring (QoM). In this work, the QoM will be related to how "good" is the visual data definition that a

camera can provide for a region located on a certain distance *dov* (distance of view). Actually, it is considered that the farther is the monitored region from the camera, the lower is the level of details related to that region in captured images, and consequently, the lower should be the amount of visual information extracted from that region. This means that the quality of captured images decreases as the distance from that camera increases, which lead us to consider different quality levels for the *FoV* of a camera. In other words, a FoV can be perceived as an area with different associated levels of monitoring quality over it.

That way, a sensor node $vs \in VS$ has its *FoV* divided into disjoint sub-regions FoV_{vs}^{l1}, FoV_{vs}^{l2} and FoV_{vs}^{l3}, which determine the visual levels 1, 2 and 3, with *high*, *medium* and *low* quality, respectively. The first level is defined by an isosceles triangle $\triangle AFG$ with its high dov_1 defined as the distance from vertex A to the end of FoV_{vs}^{l1}. The second and third levels are defined by isosceles trapezoids $\pentagon DEGF$ and $\pentagon BCED$ with highs equal to $(dov_2 - dov_1)$ and $(dov_3 - dov_2)$, respectively, as depicted in Figure 4. It is important to notice that the sensor *FoV* is not modified. It is only re-interpreted, being $FoV_{vs} = FoV_{vs}^{l1} \cup FoV_{vs}^{l2} \cup FoV_{vs}^{l3}$ and $FoV_{vs}^{l1} \cap FoV_{vs}^{l2} \cap FoV_{vs}^{l3} = \emptyset$.

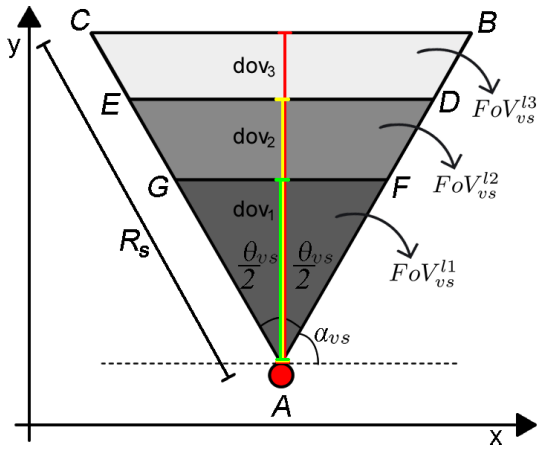

FIGURE 4. Quality perspective for a visual sensor's Field of View.

The distances dov_1, dov_2 and dov_3 can be calculated according to Equation 6 and the proportion of dov_1 and dov_2 with respect to dov_3 can be defined freely, considering the application requirements and camera's constraints. The coordinates of vertices D, E, F and G can be calculated according to Equation 7. In this article, we consider only three quality levels, but they could be extended to incorporate additional levels, without loss of generality. In fact, the quality variation will be more realistic if the same *FoV* could be divided in more quality levels.

$$\begin{aligned} dov_3 &= R_s.\cos\left(\theta_{vs}/2\right) \\ dov_2 &= \left(3/4\right) dov_3 \\ dov_1 &= \left(2/4\right) dov_3 \end{aligned} \tag{6}$$

$$\begin{aligned} \overline{AD} &= \overline{AE} = \frac{dov_2}{\cos\left(\theta_{vs}/2\right)} \\ \overline{AF} &= \overline{AG} = \frac{dov_1}{\cos\left(\theta_{vs}/2\right)} \\ D_x &= A_x + \overline{AD}.\cos\left(\alpha_{vs}\right) \\ D_y &= A_y + \overline{AD}.\sin\left(\alpha_{vs}\right) \\ E_x &= A_x + \overline{AE}.\cos\left(\left(\alpha_{vs} + \theta_{vs}\right) \bmod 2\pi\right) \\ E_y &= A_y + \overline{AE}.\sin\left(\left(\alpha_{vs} + \theta_{vs}\right) \bmod 2\pi\right) \\ F_x &= A_x + \overline{AF}.\cos\left(\alpha_{vs}\right) \\ F_y &= A_y + \overline{AF}.\sin\left(\alpha_{vs}\right) \\ G_x &= A_x + \overline{AG}.\cos\left(\left(\alpha_{vs} + \theta_{vs}\right) \bmod 2\pi\right) \\ G_y &= A_y + \overline{AG}.\sin\left(\left(\alpha_{vs} + \theta_{vs}\right) \bmod 2\pi\right) \end{aligned} \tag{7}$$

In order to provide quantitative assessment, we assign a weight value for each visual level, which is $w_1 = 1$ for FoV_{vs}^{l1}, $w_2 = 0.5$ for FoV_{vs}^{l2} and $w_3 = 0.25$ for FoV_{vs}^{l3}. Obviously, different values could be assigned, according to the application requirements. For example, following the definitions in [24], the assigned values would be $w_1 = 4$ for FoV_{vs}^{l1}, $w_2 = 2$ for FoV_{vs}^{l2} and $w_3 = 1$ for FoV_{vs}^{l3}. Actually, we use a percentage approach because an entire region "poorly" viewed would be equivalent to (a percentage) part of an "adequately" viewed region. Nevertheless, this does not mean that it is indifferent for the application to monitor a small area with good quality or a large area with low quality.

In fact, an application is probably not able to extract the same visual information from 100 *MB* poorly monitored ($w_3 = 0.25$) and from 25 *MB* well monitored ($w_1 = 1$), and vice-versa. However, we believe these quality weights are defined in a way that they can provide relevance equivalence between levels. For example, the information extracted from 25 well monitored *MB* can be as relevant as the information extracted from 100 poorly monitored *MB*, depending on the application. Actually, with less covered area, but with high coverage quality, it may be possible to make facial recognition. On the other hand, with a larger covered area, but with an associated lower coverage quality, it could be possible to detect intrusion or to perform pattern identification. Therefore, it is not necessarily about the importance of the task, but the possibility of adding value to visual information. This view-notion simplifies the understanding of the proposed metrics and indicates how practical they can be when performing quality assessment.

IV. PROPOSED QUALITY METRICS

One of the challenges to assess the monitoring quality for area coverage is the necessity to deal with continuous variations of quality in function of the distance of view of a visual sensor. But this may be a prohibitive task if it is desired to compute the QoM of the entire network instead of a single visual sensor. For that, this work treats this potential complex scenario as a discrete problem considering that the area to be monitored will be divided into monitoring blocks, thus approximating "area coverage" to the "coverage of several

targets''. In this case, the smaller the *MB*, more realistic the QoM assessment will be.

In this context, we propose three new QoM metrics: AQM, AQM_{abs} and AQM_{rel}. These Area Quality Metrics consider that, similarly to the visual levels, each monitoring block $mb \in FoV_{vs}$ receives a weight w_l which is the weight of the FoV sub-region of vs where mb can be viewed, as expressed in Equation 8.

$$w_l\,(mb, vs) = \begin{cases} w_1, & \text{if } mb \in FoV_{vs}^{l1} \\ w_2, & \text{if } mb \in FoV_{vs}^{l2} \\ w_3, & \text{if } mb \in FoV_{vs}^{l3} \end{cases} \tag{8}$$

If a monitoring block mb is redundantly covered by a set of visual sensor VS, then the weight of mb is the maximum weight among the associated sensor, as expressed in Equation 9. It is worthy to remark that in this paper it is not considered the impact of perspective of coverage. This explains why it is taken the maximum weight instead other compositions: the visual information extracted from a *MB* by different sensors will be as good as the best quality of monitoring available among the associated sensor. In a different scenario, where the coverage direction is considered, sum or average should provide a better quality representation.

$$w_{\max}\,(mb, VS) = \max\left(wl\,(mb, vs)|_{\forall vs \in VS}\right) \tag{9}$$

Figure 5 illustrates the mapping of monitoring quality of the *MB* covered by two visual sensors, including the overlapping considerations. The *MB* marked with a green circle are in *level 1* (highest quality), while the ones marked with a yellow star are in *level 2* (medium quality) and the *MB* marked with a red square are in *level 3* (lowest quality). Notice that there are some *MB* marked with more than one symbol: those *MB* are redundantly monitored by more than one visual sensor and its assigned weight is that one related to the highest quality.

We define the proposed metrics as presented in Equations 10, 11 and 12.

$$AQM_{abs}(VS) = hs \cdot ws \cdot \sum_{j=1}^{M}\sum_{l=1}^{N} w_{\max}\left(mb_{j,l}, VS\right) \tag{10}$$

$$AQM_{rel}(VS) = \frac{AQM_{abs}(VS)}{CA_{mb}\,(VS)} \tag{11}$$

$$AQM(VS) = \frac{AQM_{abs}(VS)}{h \cdot w} \tag{12}$$

The AQM_{abs} is an intermediate metric that provides an absolute perspective of the quality of monitoring, indicating the equivalent quantity of monitoring blocks. In a different way, the AQM_{rel} provides a relative perspective of the quality of monitoring, presenting the percentage of the equivalent monitoring blocks related to the covered area. Finally, AQM provides a global perspective of the quality of monitoring, indicating the percentage of the equivalent monitoring blocks related to the entire monitoring field. Actually, AQM best fits

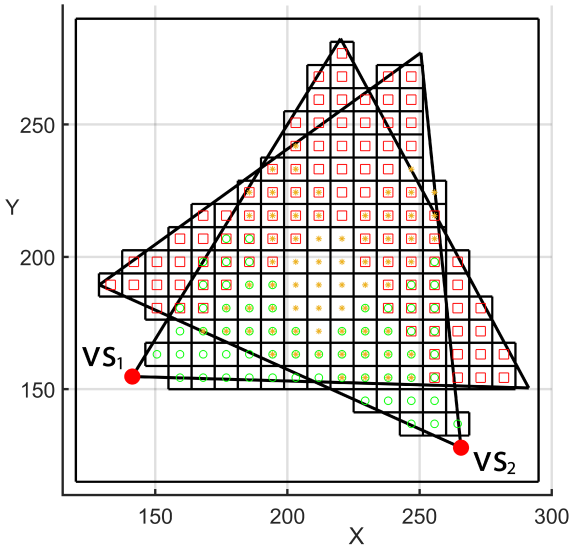

FIGURE 5. Quality of the performed area coverage when viewing monitoring blocks.

to be used as an objective function in optimization processes since it is associated with the entire monitoring field. On the other hand, AQM_{rel} reveals an innermost panorama of the coverage. A low value of AQM_{rel} ($< 62.5\%$) implies that a larger area is covered with the majority of *MB* being ''low quality'' monitored, while a high value of AQM_{rel} ($> 62.5\%$) implies that a smaller area is covered with the majority of *MB* being ''high quality'' monitored. The mean value of $AQM_{rel} = 62.5\%$ is justified because AQM_{rel} varies from 25% to 100%, which is easy to verify. In the worst case scenario, all covered *MBs* would be in the lowest quality level (w_3), which generates $AQM_{rel} = 25\%$. In the best case scenario, all covered *MBs* would be in the highest quality level (w_1), which generates $AQM_{rel} = 100\%$.

TABLE 2. QoM metrics analysis for $ws = hs = 1$.

# of covered mb			CA_{mb}	AQM_{abs}	AQM_{rel}	AQM
Lvl.1	Lvl.2	Lvl.3				
10	20	60	90	35	39%	23%
10	30	40	80	35	44%	23%
10	40	20	70	35	50%	23%
10	20	40	70	30	43%	20%
4	30	36	70	28	40%	19%

Table 2 shows fictional scenarios to better understand the meaning of the proposed metrics. The AQM is the fundamental metric, associating area coverage with the quality of monitoring. However, such monitoring can be performed on different ways. For example, a large area may be monitored with low quality, while a small area can be monitored with high quality. These two scenarios would probably present a similar AQM value, as presented in lines 1, 2 and 3 of Table 2. In those cases, it is difficult to perform

worth assessment considering only the AQM metric and thus the other proposed metrics can be used for a better perception of the considered visual sensor network.

Therefore, the AQM_{rel} appears as an auxiliary metric to help to "untie" such comparisons. Thus, it is possible to distinguish the monitoring quality between coverage schemes prioritizing area coverage (lower AQM_{rel}) or quality of monitoring (higher AQM_{rel}). The relation between these metrics can be used to improve objective functions in optimization processes. Some authors use redundancy as dependability or, specifically, as availability metrics [26], [29]. In this case, AQM_{rel} can be used to guide an optimization process focused on the maximization of quality and redundancy, for example. And the proposed metrics can be exploited to analyze and enhance quality by optimization processes and network redeployment.

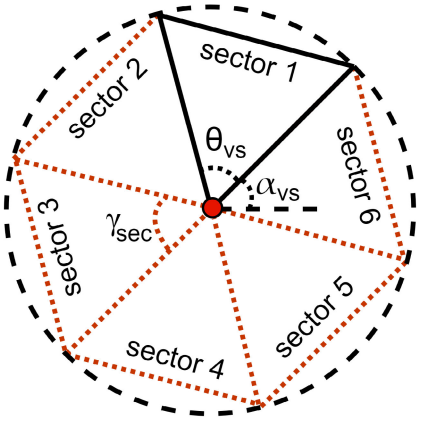

FIGURE 6. Sectors in the Greedy and Pseud-Greedy algorithms.

V. PROPOSED OPTIMIZATION ALGORITHMS

In order to illustrate the utility of the proposed metrics, three optimization algorithms are proposed aimed at the maximization of the FoV-based quality of monitoring on randomly deployed WVSN. Those optimization solutions, notably a classic greedy algorithm, a pseudo-greedy algorithm and an evolutionary algorithm, consider that visual sensors are rotatable, and so their orientations can be changed.

The proposed greedy and pseudo-greedy algorithms consider that each visual sensor may take one of a finite set of disjoint orientations. This assumption is aimed at making this problem tractable, still assuring near-optimal maximization of the quality of monitoring [26]. On the other hand, since evolutionary algorithms perform a guided random search, showing good results when seeking in a very large solution set, we consider for the proposed evolutionary algorithm that visual sensors can take any orientation.

A. GREEDY

A reasonable and feasible way to optimize the network is to compute the best orientations for each sensor individually, aiming at the maximization of covered monitoring blocks. A classical greedy heuristic looks for a global optimization, handling only local data. This is due to the complexity of dealing with global information, such as area coverage.

That way, for greedy algorithm, a visual sensor vs may assume O_{vs} different orientations (sectors), where each sector has the same angle γ_{sec}. The value of γ_{sec} can be calculated by the quantity of sectors O_{vs}, according to Equation 13.

$$\gamma_{sec} = \lfloor 360^o / O_{vs} \rfloor \tag{13}$$

Therefore, for each sector $o = 1, \ldots, O_{vs}$, the possible new orientation of vs will be α^o_{vs}, according to Equation 14 (as shown in Figure 6, where $\gamma_{sec} = \theta_{vs} = 60°$), where α_{vs} is the original orientation of vs.

$$\alpha^o_{vs} = (o-1) \times \gamma_{sec} + \alpha_{vs} \tag{14}$$

The proposed Greedy approach is based on individually testing which orientation provides the highest QoM for each single visual sensor, then redeploying the sensor for that orientation. In this case, each sensor node will be re-orientated in order to compute the highest AQM. Actually, this is a simple way to improve the value of QoM, while keeping lower computational costs as compared with other approaches, although greedy algorithms may provide sub-optimal results since they only evaluate local information [30]. The proposed Greedy approach is detailed in Algorithm 1.

It is worth to remark that, since this approach only analyzes each sensor individually, it is not possible to guide the optimization directly by the metric AQM. However, it is important to present this method to realize the premise of quality optimization and to have a basis of comparison. In spite of that, one should notice that a notion of QoM is provided by the variable $SensorQoM$ (Algorithm 1, Line 17), which is the quality perceived by a single visual sensor.

B. PSEUDO-GREEDY

The main disadvantage of the Greedy approach is to use only local information at the optimization process. To cope with that problem, we propose a Pseudo-Greedy algorithm based on [26], but here aiming at QoM optimization instead of dependability optimization. This approach keeps looking for a global optimum while searching in local solutions, but in a different way of a classic Greedy approach, it uses some global information recovered in a lightweight way to improve the searching process. The idea is to re-orientate each sensor node in a way that it generates the highest overall quality of monitoring instead of the highest quality possible by the sensor. Algorithm 2 shows the proposed Pseudo-Greedy heuristic.

The first step is to identify, for each visual sensor node, its covered monitoring blocks (Line 3) and store the associated weight value (Line 4). Then, iteratively, each sensor (one at time) is re-orientated to the position that generates the highest QoM considering the current position of the other sensors. For this, it is generated a finite set of sectors,

Algorithm 1 Proposed Greedy Optimization Algorithm

Data: $\boldsymbol{VS}$ = Greedy($\boldsymbol{VS}$, $\boldsymbol{MA}$, O_{vs});
Input: List of sensors, monitoring area parameters and number of sectors.
Output: A set of reoriented visual sensors $\boldsymbol{VS}$.

1 **foreach** *visual sensor* **vs** *in sensors set* $\boldsymbol{VS}$ **do**
2 angles = [];
3 $\gamma_{sec} = \lfloor 360^o / O_{vs} \rfloor$;
4 $\alpha' = vs.\alpha$;
5 **foreach** *sector* $o = 1, \ldots, O_{vs}$ **do**
6 MB = [];
7 $\alpha^o_{vs} = (o-1) \times \gamma_{sec} + \alpha'$;
  // Re-orientate *vs* with α^o_{vs}
8 $vs.\alpha = \alpha^o_{vs}$;
9 **foreach** *Monitoring Block* $\boldsymbol{mb}_{j,l}$ **do**
10 **if** *isCovered*($\boldsymbol{mb}_{j,l}$) **then**
11 MB[j,l] = $w_l(mb_{j,l}, vs)$;
12 **end**
13 **else**
14 MB[j,l] = 0;
15 **end**
16 **end**
17 SensorQoM = sum(MB);
18 angles.add({α^o_{vs}, SensorQoM}) ;
19 **end**
20 $vs.\alpha$ = angles.getMaxSensorQoM();
21 **end**
22 **return** $\boldsymbol{VS}$;

Algorithm 2 Proposed Pseudo-Greedy Algorithm

Data: $\boldsymbol{VS}$ = pseudoGreedy($\boldsymbol{VS}$, $\boldsymbol{MA}$), O_{vs});
Input: List of sensors, monitoring area parameters and number of sectors.
Output: A set of reoriented visual sensors $\boldsymbol{VS}$.

1 **foreach** *visual sensor* **vs** *in sensors set* $\boldsymbol{VS}$ **do**
2 **foreach** *Monitoring Block* $\boldsymbol{mb}_{j,l}$ **do**
  // Create a matrix MB[] of covered
  // monitoring blocks per visual sensor
3 **if** *isCovered*($\boldsymbol{mb}_{j,l}$) **then**
4 MB[j,l,vs] = $w_l(mb_{j,l}, vs)$;
5 **end**
6 **else**
7 MB[j,l,vs] = 0;
8 **end**
9 **end**
10 **end**
11 k=0; angles = []; $\text{angles}_{Err} = \infty$;
12 **while** $\text{angles}_{Err} > \epsilon$ && $k{+}{+} < |\boldsymbol{VS}|$ **do**
13 **foreach** *visual sensor* **vs** *in sensors set* $\boldsymbol{VS}$ **do**
14 $\gamma_{sec} = \lfloor 360^o / O_{vs} \rfloor$;
15 $\alpha' = vs.\alpha$;
16 **foreach** *sector* $o = 1, \ldots, O_{vs}$ **do**
  // Re-orientate *vs* with α^o_{vs}
17 $\alpha^o_{vs} = (o-1) \times \gamma_{sec} + \alpha'$;
18 $vs.\alpha = \alpha^o_{vs}$;
19 update(MB[:, :, vs]);
20 MB'[] = max (MB[:, :, :]);
21 AQM_{abs} = $hs \times ws \times$ sum (MB');
22 $AQM = AQM_{abs} / (h \times w)$;
23 angles.add({α^o_{vs}, AQM}) ;
24 **end**
25 $vs.\alpha$ = angles.getMaxAQM();
26 update(MB[:, :, vs]);
27 **end**
28 $\text{angles}_{Err} = abs(\text{angles}(k) - \text{angles}(k-1))$;
29 **end**
30 **return** $\boldsymbol{VS}$;

which are disjoint possible orientations to be assumed by the visual sensor (Line 14). For each sector to be tested, it is identified the *MB* covered by the sensor in its new orientation, storing the associated weight value according to Equation 8 (Line 19). Then, the *AQM* is computed considering the new orientation of *vs*. Each computed value of *AQM* is stored (Line 23) and the orientation which generates the highest quality is associated to the sensor (Line 25). This procedure is repeated for each sensor until the network assumes a convergent deployment configuration. Since the computing of the *AQM* is basically the summing of all elements in a matrix (Lines 21 and 22), this step adds valuable global information to the optimization process without computational overhead.

C. EVOLUTIONARY

In order to search in a vaster solutions space, we also implemented an evolutionary optimization process based on Genetic Algorithms. These algorithms perform a guided random search, inspired on natural evolution concepts such as survival of the fittest, crossover and mutation. The randomness of the algorithm makes it a good approach to look for optimal or near-optimal combinations of solutions that might not otherwise be found in a lifetime. However, such approach presents a relatively high computational complexity, which may be prohibitive for some scenarios. Since we provide a lightweight heuristic to compute QoM, Genetic Algorithms became a feasible solution. Figure 7 shows the steps sequence of these algorithms.

The execution starts with an initial population, which is the original deployment configuration, and some eligible solutions randomly generated. A chromosome belonging to the population is a set containing the orientation α_{vs} of each visual node. This population is evaluated (fitness) in order to identify which chromosomes best fit as solution for the

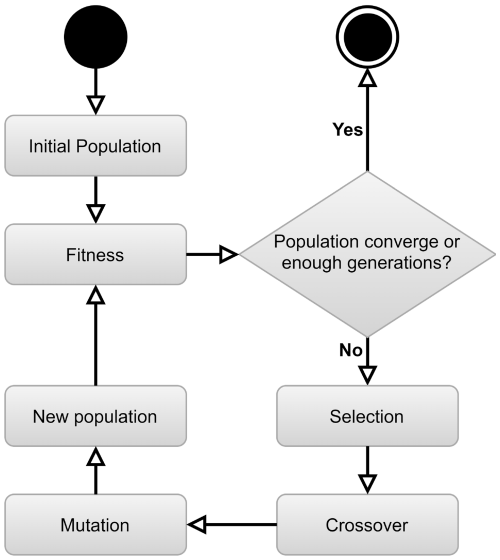

FIGURE 7. Flowchart of typical Genetic Algorithms.

optimization problem. Therefore, the fitness phase computes the *AQM* generated by all visual nodes together. In the next step, some chromosomes are selected as parents that mate and recombine to create off-springs for the next generation. We use a proportional selection based on Roulette Wheel, *i.e.*, each individual can become a parent with a probability proportional to its fitness, but not necessarily the best chromosomes are chosen [31]. To avoid that, we also apply elitist selection, which directly copy the best chromosome to the new population in the next generation. Then, a crossover is performed, when some chromosomes pair and exchange part of their DNA, which means that some visual sensors from different solutions exchange their orientations. A few visual sensors can also suffer mutation and change their orientation randomly. Crossover and mutation operators are crucial to provide a more diverse population in order to make the heuristic more immune to be trapped in a local optima. Finally, elite and selected chromosomes join new chromosomes that are randomly generated to produce a new population. The process is repeated until it fulfills the stopping criterion, which could be a maximum number of generations or the fitness convergence [32].

VI. NUMERICAL RESULTS

In this section, some analysis and numerical results related to the utilization of the proposed metrics are presented. Initially, we analyze the impact of the viewing angle on each *FoV* level, considering constant values of dov_1, dov_2 and dov_3. Then, in order to improve the QoM of a network, the three proposed optimization algorithms are compared regarding maximization of the *AQM*, and their performances are analyzed and discussed. We also show how the metrics *AQM* and AQM_{rel} are associated and how they can be used together to analyze the QoM perception. Algorithms and designed simulations were implemented in the Mathworks MATLAB platform.

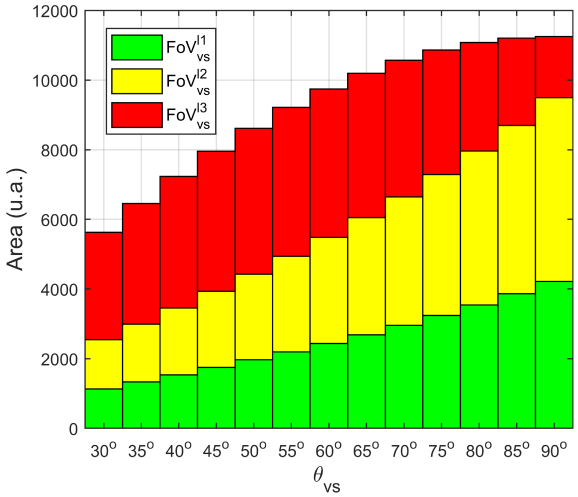

FIGURE 8. Quality variation related to the viewing angle.

A. EXPERIMENTAL SETTINGS

For the performed simulations, the same configuration is considered, with all visual sensors having the same sensing radius $R_s = 150$ units of distance (*u.d.*). As a reference when setting the viewing angle, Figure 8 shows the total covered area by a visual node, as well as the covered area by each *FoV* level. It can be seen that for smaller angles (below 45°) we have lower covered area. For 75° and higher we have a greater covered area, specially for FoV^{l1}_{vs} and FoV^{l2}_{vs}. However, very wide angles bring the risk of loss of quality on peripheral areas. This could be solved increasing the image definition or setting an anisotropic QoM with respect to viewing angle [13]. That being said, we set $\theta_{vs} = 60°$ which is an intermediate value and also it is the average viewing angle of several commercial cameras widely used on academy and industry, such as *RaspiCam* and *Cisco IP cameras* [7]. These visual nodes must cover a monitoring area with $w = 500$ *u.d.*, $h = 500$ *u.d.*, $ws = hs = 8.5$ *u.d.* and $\beta = 0°$, which are the same values used in [26]. The position and orientation of each sensor node were randomly generated. The position is limited to 100 *u.d.* away from monitoring area at most, since there is no point to place a visual sensor too far that cannot be able to cover the area of interest.

For the first test, in each simulation, all three proposed algorithms were executed. The Greedy and the Pseudo-Greedy algorithms divide the search space into 30 sectors, while the Evolutionary approach handles 50 chromosomes over 100 generations, with crossover and mutation probabilities of 0.7 and 0.01, respectively. In this scenario, 600 simulations were performed, being 100 simulations for each scenario that vary the number of visual sensors, *i.e.*, scenarios with 5, 10, 20, 30, 40, 50 visual sensors. This way, the impact of the quantity of visual sensors and redundancy on the QoM could be analyzed.

B. OPTIMIZATION COMPARISON

For each scenario, we took the average values from each group of 100 simulations. Figures 9 and 10 show the gain

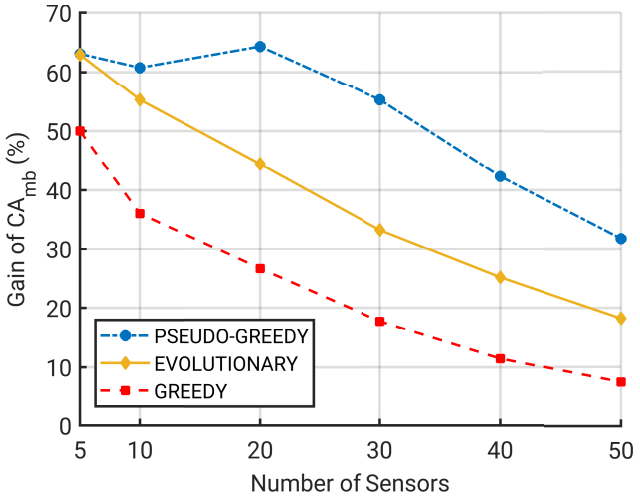

FIGURE 9. Area coverage improvement.

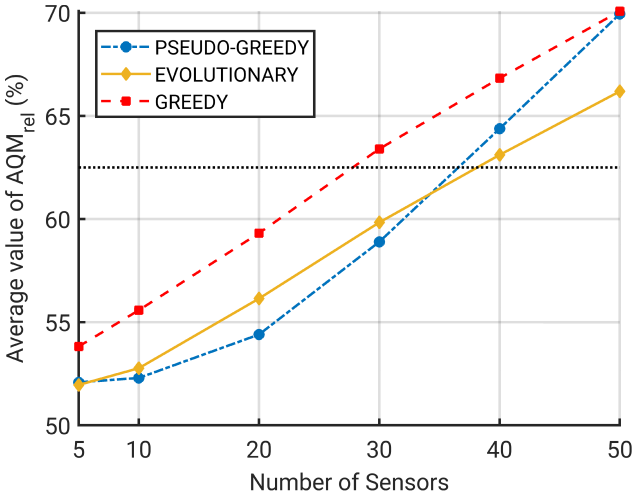

FIGURE 11. Average value of AQM_{rel}.

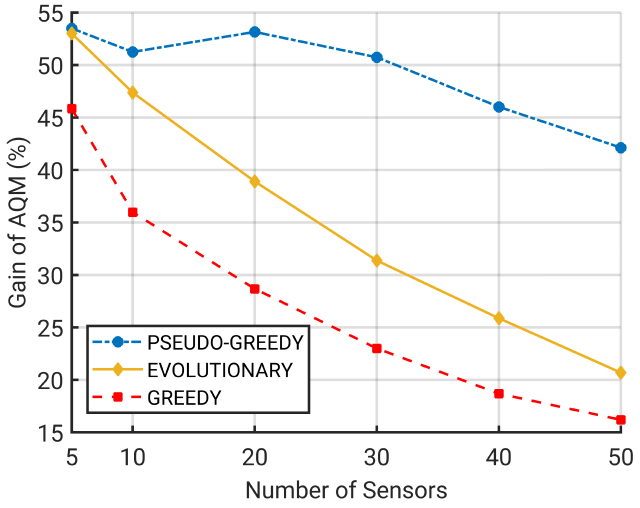

FIGURE 10. *AQM* improvement.

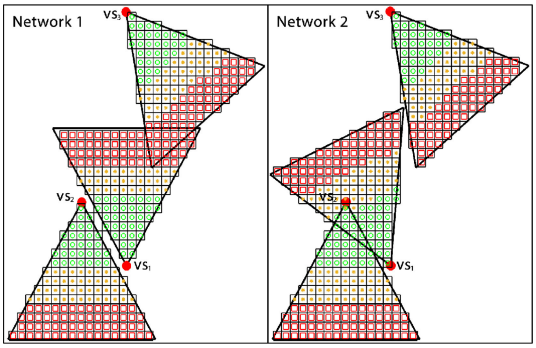

FIGURE 12. Association between covered area and QoM.

of area coverage and of *AQM* provided by each optimization algorithm in relation to the initial deployment. Since AQM_{rel} is a relative metric, it does not make sense to present its gain. Instead, Figure 11 presents the average value of AQM_{rel} from executed simulations. As shown in Figure 9, all optimization methods provide a considerable gain of the total covered area that is reflected on the number of *MBs* covered. Comparing this result with Figure 10, it is possible to see that all optimization methods also provide a considerable gain of *AQM* at the same order: the Pseudo-Greedy algorithm provides a higher gain than the Evolutionary, which provides a higher gain than the Greedy. This is due to the fact that the Greedy algorithm only considers local information and in a limited search space, while the Evolutionary approach has and infinite search space, but exploited by a random guided search using information of the entire network. Finally, the Pseudo-Greedy algorithm also exploits information from other nodes, but using a deterministic search.

For a small number of visual sensor nodes (5 to 20, in the case of monitoring network configurations taken as example) there is plenty of uncovered regions which provides "room for improvement" to the optimization algorithms, generating high gains in Figures 9 and 10. As the number of visual sensors increases (30 to 50), uncovered regions shrink and these gains decrease. It does not mean that the QoM decreases. On the contrary, the optimization process keeps increasing the perception of quality (QoM) and the coverage area.

Furthermore, it is worthy to discuss the evolutionary results since that approach is generally applied to complex problems providing good solutions. However, in this work, it did not provide the best results. The main explanation to this discrepancy between the expected and obtained results is that the evolutionary approach could eventually find the same result or better than other approaches, since it has a wider solutions space. However, it may take much more time than the acceptable timeout that we set at the algorithm searching parameters for 50 chromosomes through 100 generations. It could eventually happen in the simulations, but it will hardly appear at the results since we are taking the average value from 100 simulations. This is, in fact, a reason to

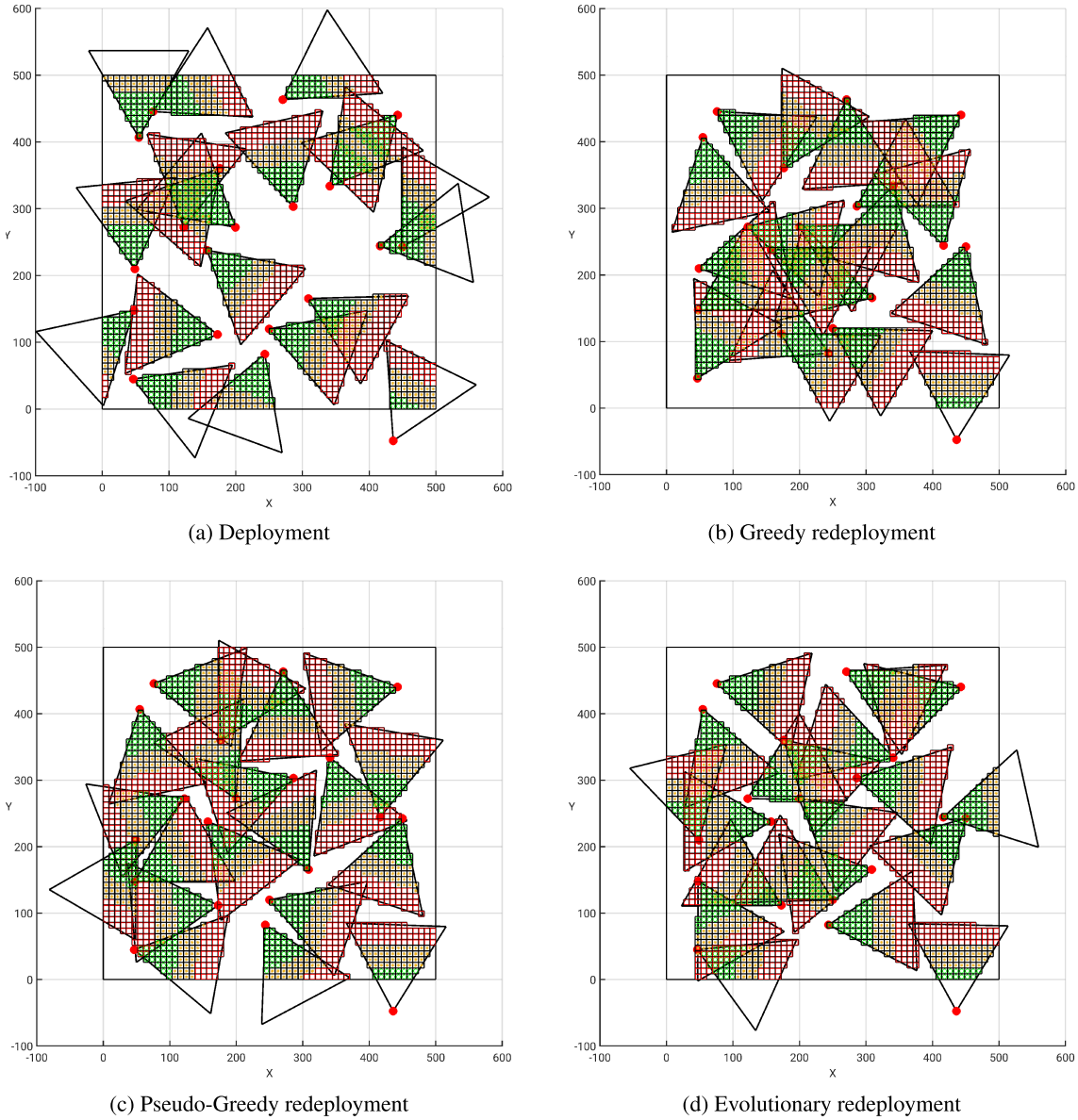

(a) Deployment

(b) Greedy redeployment

(c) Pseudo-Greedy redeployment

(d) Evolutionary redeployment

FIGURE 13. Example of a WVSN and the respective redeployment by each optimization algorithm.

exalt the Pseudo-Greedy results: it is so fast and efficient in this context that overcomes the evolutionary approach results. As a final remark, the simulations showed that the Pseudo-Greedy optimization method converges in only 4 iterations, in average.

Considering the AQM_{rel} metric, in Figure 11 the networks with higher relative quality of monitoring, *i.e.*, with more *MBs* "well" viewed (*MBs* in majority inside of FoV_{vs}^{l1} and FoV_{vs}^{l2}), were redeployed by the Greedy optimization with more than 30 sensors, or by the Pseudo-Greedy and Evolutionary optimization with more then 40 sensors, since they present $AQM_{rel} \geq 62.5\%$. This means that, even if these redeployments do not provide the highest amount of covered area or the highest AQM, the available visual information is assumed as having high quality and it can be used for more specialized tasks.

C. QUALITY OF MONITORING VS. AREA COVERAGE

Another interesting result to notice is that the growth of covered area (Figure 9) followed by the growth of the AQM (Figure 10) in this comparison could leave the wrong impression that the area coverage optimization (area maximization or redundancy minimization) directly leads to QoM optimization. But it may be not true in many cases. Actually, it is natural that, increasing the covered area after an optimization process, more non-monitored regions will be encompassed, which tends to contribute to the gathering of more visual data and the improvement of the QoM perception. However, a non-optimal area coverage could provide less overlapping of regions with the same weight, providing a higher QoM. An example of this phenomenon can be seen in Figure 12. In this case, the first network presents $CA_{mb}(VS) = 28835$ and $AQM_{abs}(VS) = 14529$,

while the second network presents $CA_{mb}(VS) = 28166$ $AQM_{abs}(VS) = 14696$. Hence, the network 1 has a higher covered area and a lower QoM than network 2. This means that we can not reduce the problem of QoM optimization to a simple area coverage maximization or redundancy minimization.

We investigated this issue more carefully and implemented the Greedy, Pseudo-Greedy end Evolutionary optimization processes aiming at area coverage maximization, according to [26]. Then, the results were compared with the optimization aiming at QoM maximization in each simulation. It could be seen that only in 24% of the simulations, the area coverage maximization implied in QoM maximization, which justifies the metrics and algorithms proposed in this article.

D. QUALITY OF MONITORING ASSESSMENT EXAMPLE

In order to illustrate the discussion stated from the optimization methods, Figure 13 shows an example of distribution of visual sensors on the initial deployment and after the execution of the Greedy, the Pseudo-Greedy and the Evolutionary redeployment algorithms in a WVSN with 20 visual nodes. Table 3 presents the covered area and the quality metrics related to each (re)deployment. As suggested by the graphics in Figures 9 and 10, the Pseudo-Greedy optimization provides a higher covered area as well as higher QoM. It is worthy to remark that these high values for the metrics may imply in an unconventional redeployment. For example, in Figures 13c and 13d this is achieved orientating some sensors in a way that their *FoV* are outside of the monitoring area. This also explains the reason for the Greedy optimization to provide a higher AQM_{rel}: there is higher area coverage redundancy, specially for FoV_{vs}^{l3} and FoV_{vs}^{l2} (see Figure 13b).

TABLE 3. Quality metrics for the results in Figure 13.

(Re)Deployment	Covered Area (u.a)	AQM	AQM_{rel}
Initial	127972	29.8%	58.2%
Greedy	142018	33.5%	59%
Evolutionary	146626	33.9%	57.8%
Pseudo-Greedy	165131	36.6%	55.5%

VII. CONCLUSIONS

This article discussed the quality of monitoring in wireless visual sensors networks when performing area coverage. Quality was addressed based on the characteristics of the sensor's *FoV*, but such perception of quality was also exploited as an attribute of the entire visual sensor network. In this context, metrics were proposed for both cases, providing a practical mathematical tool for quality assessment. Actually, this network quality model is more realistic than others found in the literature, since it does not enforce predefined camera's position or orientation and provide high flexibility on several parameters, such as quantity and width of quality levels.

In this article, we have shown how to analyze the features of a network based on QoM metrics and how to use those metrics to improve the quality of monitoring through three proposed optimization algorithms. Also, this work showed the importance of metrics to perform mathematical analysis related to the utility of available visual information with respect to the perceived QoM, as well as the potential to exploit other quality aspects, such as dependability or redundancy.

The presented numerical results reinforce the idea that the proposed metrics indicate valuable information of the networks, being possible to distinguish QoM among several distinct networks deployments. Additionally, the optimization algorithms achieved good results, specially the Pseudo-Greedy, which increased the QoM up to 54% and area coverage up to 65%. The relationship between QoM and area coverage was also studied and we showed that they are not directly related, which justifies the metrics and algorithms proposed in this article.

Finally, the ideas and insights discussed in this work, although consistent, still demand additional investigation and potentially new proposals. In fact, new quality levels considering an anisotropic perspective, dealing properly with too oblique viewing angles or with peripheral regions, might bring even more realism to the proposed model. Another improvement could be the inclusion of dynamic external factors that affect the perceived QoM, such as incidence or lack of luminosity, or even weather conditions like fog, rain, snow and dust. At last, other future works could also analyze the network dependability as a function of QoM, further associating visual quality to the network availability.

REFERENCES

[1] F. G. H. Yap and H.-H. Yen, "A survey on sensor coverage and visual data capturing/processing/transmission in wireless visual sensor networks," *Sensors*, vol. 14, no. 2, pp. 3506–3527, 2014.

[2] P. Dolezel and D. Honc, "Neural network for smart adjustment of industrial camera—Study of deployed application," in *AETA-Recent Advances in Electrical Engineering and Related Sciences: Theory and Application*, I. Zelinka, P. Brandstetter, T. T. Dao, V. H. Duy, and S. B. Kim, Eds. Cham, Switzerland: Springer, 2020, pp. 101–113.

[3] Y. Balouin, H. Rey-Valette, and P.-A. Picand, "Automatic assessment and analysis of beach attendance using video images at the Lido of Sète beach, France," *Ocean Coastal Manage.*, vol. 102, pp. 114–122, Dec. 2014.

[4] L. F. Bittencourt, J. Diaz-Montes, R. Buyya, O. F. Rana, and M. Parashar, "Mobility-aware application scheduling in fog computing," *IEEE Cloud Comput.*, vol. 4, no. 2, pp. 26–35, Mar./Apr. 2017.

[5] S. Y. Jang, Y. Lee, B. Shin, and D. Lee, "Application-aware IoT camera virtualization for video analytics edge computing," in *Proc. IEEE/ACM Symp. Edge Comput. (SEC)*, Oct. 2018, pp. 132–144.

[6] T. C. Jesus, P. Portugal, F. Vasques, and D. G. Costa, "Automated methodology for dependability evaluation of wireless visual sensor networks," *Sensors*, vol. 18, no. 8, p. 2629, 2018.

[7] D. G. Costa, "Visual sensors hardware platforms: A review," *IEEE Sensors J.*, vol. 20, no. 8, pp. 4025–4033, Apr. 2020.

[8] Z. Wang, A. C. Bovik, H. R. Sheikh, and E. P. Simoncelli, "Image quality assessment: From error visibility to structural similarity," *IEEE Trans. Image Process.*, vol. 13, no. 4, pp. 600–612, Apr. 2004.

[9] X. Min, K. Gu, G. Zhai, J. Liu, X. Yang, and C. W. Chen, "Blind quality assessment based on pseudo-reference image," *IEEE Trans. Multimedia*, vol. 20, no. 8, pp. 2049–2062, Aug. 2018.

[10] H. Duan, G. Zhai, X. Min, Y. Zhu, Y. Fang, and X. Yang, "Perceptual quality assessment of omnidirectional images," in *Proc. IEEE Int. Symp. Circuits Syst. (ISCAS)*, May 2018, pp. 1–5.

[11] Y. Zhu, G. Zhai, X. Min, and J. Zhou, "The prediction of saliency map for head and eye movements in 360 degree images," *IEEE Trans. Multimedia*, early access, Dec. 12, 2019, doi: 10.1109/TMM.2019.2957986.
[12] D. G. Costa, L. A. Guedes, F. Vasques, and P. Portugal, "QoV: Assessing the monitoring quality in visual sensor networks," in *Proc. IEEE 8th Int. Conf. Wireless Mobile Comput. Netw. Commun. (WiMob)*, Oct. 2012, pp. 667–674.
[13] W. Wang, H. Dai, C. Dong, F. Xiao, X. Cheng, and G. Chen, "VISIT: Placement of unmanned aerial vehicles for anisotropic monitoring tasks," in *Proc. 16th Annu. IEEE Int. Conf. Sens., Commun., Netw. (SECON)*, Jun. 2019, pp. 1–9.
[14] H. Yang, D. Li, and H. Chen, "Coverage quality based target-oriented scheduling in directional sensor networks," in *Proc. IEEE Int. Conf. Commun.*, May 2010, pp. 1–5.
[15] X. Ren, W. Liang, and W. Xu, "Quality-aware target coverage in energy harvesting sensor networks," *IEEE Trans. Emerg. Topics Comput.*, vol. 3, no. 1, pp. 8–21, Mar. 2015.
[16] S. Hanoun, A. Bhatti, D. Creighton, S. Nahavandi, P. Crothers, and C. G. Esparza, "Target coverage in camera networks for manufacturing workplaces," *J. Intell. Manuf.*, vol. 27, no. 6, pp. 1221–1235, 2016.
[17] S. Tang and J. Yuan, "DAMson: On distributed sensing scheduling to achieve high quality of monitoring," in *Proc. IEEE INFOCOM*, Apr. 2013, pp. 155–159.
[18] L. Guo, D. Li, Y. Zhu, D. Kim, Y. Hong, and W. Chen, "Enhancing barrier coverage with β quality of monitoring in wireless camera sensor networks," *Ad Hoc Netw.*, vol. 51, pp. 62–79, Nov. 2016.
[19] J. Huang, C. Lin, X. Kong, B. Wei, and X. Shen, "Modeling and analysis of dependability attributes for services computing systems," *IEEE Trans. Serv. Comput.*, vol. 7, no. 4, pp. 599–613, Oct. 2014.
[20] T. C. Jesus, D. G. Costa, P. Portugal, F. Vasques, and A. Aguiar, "Modelling coverage failures caused by mobile obstacles for the selection of faultless visual nodes in wireless sensor networks," *IEEE Access*, vol. 8, pp. 41537–41550, 2020.
[21] D. G. Costa, I. Silva, L. A. Guedes, P. Portugal, and F. Vasques, "Availability assessment of wireless visual sensor networks for target coverage," in *Proc. Emerg. Technol. Factory Automat. (ETFA)*, Sep. 2014, pp. 1–8.
[22] H. Zannat, T. Akter, M. Tasnim, and A. Rahman, "The coverage problem in visual sensor networks: A target oriented approach," *J. Netw. Comput. Appl.*, vol. 75, pp. 1–15, Nov. 2016.
[23] P. Fu, Y. Cheng, H. Tang, B. Li, J. Pei, and X. Yuan, "An effective and robust decentralized target tracking scheme in wireless camera sensor networks," *Sensors*, vol. 17, no. 3, p. 639, 2017.
[24] J. Tao, T. Zhai, H. Wu, Y. Xu, and Y. Dong, "A quality-enhancing coverage scheme for camera sensor networks," in *Proc. 43rd Annu. Conf. IEEE Ind. Electron. Soc.*, Oct. 2017, pp. 8458–8463.
[25] Y. Hu, X. Wang, and X. Gan, "Critical sensing range for mobile heterogeneous camera sensor networks," in *Proc. IEEE Conf. Comput. Commun. (IEEE INFOCOM)*, Apr. 2014, pp. 970–978.
[26] T. C. Jesus, D. G. Costa, and P. Portugal, "Wireless visual sensor networks redeployment based on dependability optimization," in *Proc. IEEE 17th Int. Conf. Ind. Inform. (INDIN)*, Jul. 2019, pp. 1111–1116.
[27] D. G. Costa, C. Duran-Faundez, and J. C. N. Bittencourt, "Availability issues for relevant area coverage in wireless visual sensor networks," in *Proc. Conf. Electr., Electron. Eng., Inf. Commun. Technol. (CHILEAN)*, Oct. 2017, pp. 1–6.
[28] T. C. Jesus, D. G. Costa, and P. Portugal, "On the computing of area coverage by visual sensor networks: Assessing performance of approximate and precise algorithms," in *Proc. IEEE 16th Int. Conf. Ind. Inform. (INDIN)*, Jul. 2018, pp. 193–198.
[29] C. Istin, D. Pescaru, and H. Ciocarlie, "Performance improvements of video WSN surveillance in case of traffic congestions," in *Proc. Int. Joint Conf. Comput. Cybern. Tech. Inform.*, May 2010, pp. 659–663.
[30] D. G. Costa, E. Rangel, J. P. J. Peixoto, and T. C. Jesus, "An availability metric and optimization algorithms for simultaneous coverage of targets and areas by wireless visual sensor networks," in *Proc. IEEE 17th Int. Conf. Ind. Inform. (INDIN)*, Jul. 2019, pp. 617–622.
[31] A. Shukla, H. M. Pandey, and D. Mehrotra, "Comparative review of selection techniques in genetic algorithm," in *Proc. Int. Conf. Futuristic Trends Comput. Anal. Knowl. Manage. (ABLAZE)*, 2015, pp. 515–519.
[32] H. Wei and X.-S. Tang, "A genetic-algorithm-based explicit description of object contour and its ability to facilitate recognition," *IEEE Trans. Cybern.*, vol. 45, no. 11, pp. 2558–2571, Nov. 2015.

THIAGO C. JESUS received the B.Sc. degree in computer engineering from the State University of Feira de Santana, Brazil, in 2008, and the M.Sc. degree in electrical engineering from the Federal University of Rio de Janeiro, Brazil, in 2011. He is currently pursuing the Ph.D. degree in electrical and computer engineering program with the Faculty of Engineering, University of Porto, Portugal.

He is also an Auxiliary Professor with the Department of Technology, State University of Feira de Santana. He is the author or coauthor of several articles. His research interests include dependability evaluation on wireless sensor networks, fault diagnosis of discrete event systems, industrial communication systems, and smart cities. He acted as a reviewer for high-quality journals in those areas.

DANIEL G. COSTA (Senior Member, IEEE) received the B.Sc. degree in computer engineering and the M.Sc. and D.Sc. degrees in electrical engineering from the Federal University of Rio Grande do Norte, Brazil, in 2005, 2006, and 2013, respectively.

He did his research internship with the University of Porto, Portugal. He is currently an Associate Professor with the Department of Technology, State University of Feira de Santana, Brazil. He is also with the Advanced Networks and Applications Laboratory, LARA, State University of Feira de Santana. He is the author or coauthor of more than 100 articles in the areas of computer networks, industrial communication systems, the Internet of Things, smart cities, and sensor networks. He has served several number of committees of distinguished international conferences. He acted as a reviewer for high-quality journals.

PAULO PORTUGAL (Member, IEEE) received the Ph.D. degree in electrical and computer engineering from the Faculty of Engineering (FEUP), University of Porto (UP), Porto, Portugal, in 2005. He is currently an Associate Professor with the Electrical and Computer Engineering Department (DEEC), FEUP, UP. His current research interests include industrial communications and dependability/performability modeling.

FRANCISCO VASQUES received the Ph.D. degree in computer science from LAAS-CNRS, Toulouse, France, in 1996.

Since 2004, he has been an Associate Professor with the University of Porto, Portugal. He is the author or coauthor of more than 150 articles in the areas of real-time systems and industrial communication systems. His current research interests include real-time communication, industrial communication, and real-time embedded systems. He has been also a member of the Editorial Board of *Sensors* (MDPI), *Sensor Networks Section* (MDPI), since 2018, and the *International Journal of Distributed Sensor Networks* (Hindawi). Since 2007, he has been an Associate Editor of the IEEE TRANSACTIONS ON INDUSTRIAL INFORMATICS for the topic Industrial Communications.